Acta Biomaterialia xxx (2014) xxx–xxx

Contents lists available at ScienceDirect

Acta Biomaterialia

journal homepage: www.elsevier.com/locate/actabiomat

A biomimetic multi-layered collagen-based scaffold for osteochondral repair

Tanya J. Levingstone [a,b,c], Amos Matsiko [a,b,c], Glenn R. Dickson [a], Fergal J. O'Brien [a,b,c,*], John P. Gleeson [a,b,c,d]

[a] Tissue Engineering Research Group, Department of Anatomy, Royal College of Surgeons in Ireland, Dublin, Ireland
[b] Trinity Centre for Bioengineering, Dublin, Ireland
[c] Advanced Materials and Bioengineering Research (AMBER) Centre, Royal College of Surgeons in Ireland and Trinity College Dublin, Dublin, Ireland
[d] SurgaColl Technologies Ltd, Rubicon Centre, Rossa Avenue, Cork, Ireland

ARTICLE INFO

Article history:
Received 8 August 2013
Received in revised form 19 December 2013
Accepted 2 January 2014
Available online xxxx

Keywords:
Collagen
Osteochondral defects
Cartilage tissue engineering
Multi-layered scaffolds

ABSTRACT

Cartilage and osteochondral defects pose a significant challenge in orthopedics. Tissue engineering has shown promise as a potential method for the treatment of such defects; however, a long-lasting repair strategy has yet to be realized. This study focuses on the development of a layered construct for osteochondral repair, fabricated through a novel "iterative layering" freeze-drying technique. The process involved repeated steps of layer addition followed by freeze-drying, enabling control over material composition, pore size and substrate stiffness in each region of the construct, while also achieving a seamlessly integrated layer structure. The novel construct developed mimics the inherent gradient structure of healthy osteochondral tissue: a bone layer composed of type I collagen and hydroxyapatite (HA), an intermediate layer composed of type I collagen, type II collagen and HA and a cartilaginous region composed of type I collagen, type II collagen and hyaluronic acid. The material properties were designed to provide the biological cues required to encourage infiltration of host cells from the bone marrow while the biomechanical properties were designed to provide an environment optimized to promote differentiation of these cells towards the required lineage in each region. This novel osteochondral graft was shown to have a seamlessly integrated layer structure, high levels of porosity (>97%), a homogeneous pore structure and a high degree of pore interconnectivity. Moreover, homogeneous cellular distribution throughout the entire construct was evident following *in vitro* culture, demonstrating the potential of this multi-layered scaffold as an advanced strategy for osteochondral defect repair.

1. Introduction

Osteochondral defects, involving the smooth cartilage lining of the articulating surface and the underlying subchondral bone, frequently occur due to disease or as a result of traumatic injury to the joint [1]. Due to the body's extremely limited capacity to repair such defects, the prognosis is chronic degradation, and surgical intervention is frequently required [2]. The treatment options depend on factors such as age, lesion diameter and depth, and location within the joint [3,4]. Autologous osteochondral grafting is currently recognized as the clinical gold standard for the treatment of osteochondral defects. However, this technique possesses many inherent limitations, including donor site morbidity and limited quantity of suitable host tissue, as well as the difficulty in correctly matching the topography of the graft with the healthy tissue surrounding the defect site [5]. Issues including incomplete integration between the host tissue and graft tissue [6] and the degradation of the graft tissue are often observed [7]. Tissue engineering (TE) strategies may provide significant advantages compared to these more traditional clinical treatment methods. Two approaches are typically used: (i) cell-free scaffolds, an approach which relies on the principle that the patient's own cells infiltrate into the scaffold and subsequently synthesize repair tissue; and (ii) cell-seeded scaffolds, whereby cells are harvested from the patient and cultured *in vitro* on a scaffold prior to implantation. In both situations, the properties of the scaffold, including porosity, pore size [8,9] and substrate stiffness [10,11], are known to be key determinants which influence cellular attachment, infiltration and lineage specification of mesenchymal stem cells (MSCs).

While cell-seeded approaches tend to place less focus on the scaffolds and rely mainly on the delivered cells to engineer the repair tissue, cell-free scaffolds used in osteochondral TE place particular emphasis on the composition and structure of the scaffold. This is done in an effort to provide an environment that can

* Corresponding author at: Tissue Engineering Research Group, Department of Anatomy, Royal College of Surgeons in Ireland, 123 St Stephen's Green, Dublin 2, Ireland. Tel.: +353 1 402 2149; fax: +353 1 402 2355.
E-mail address: fjobrien@rcsi.ie (F.J. O'Brien).

1742-7061/$ - see front matter © 2014 Acta Materialia Inc. Published by Elsevier Ltd. All rights reserved.
http://dx.doi.org/10.1016/j.actbio.2014.01.005

support the existing host cell population, thereby circumventing the costly and cumbersome requirement of *in vitro* pre-culture prior to implantation. Numerous scaffolds utilized in this area consist of synthetic materials, such as poly(e-caprolactone) (PCL) [12], poly(glycolic acid) (PGA) [13] and poly(lactide-co-glycolide) (PLGA) [14,15]. However, slow degradation rates, harmful degradation by-products, poor cell attachment, an inability to direct cellular differentiation and reduced immunogenicity have led to limited long-term success following *in vivo* application [13]. Natural materials, including collagen [16,17] fibrin [18], hyaluronan [19], alginate [20] and agarose [21–23], have been widely investigated for use in osteochondral tissue repair. Of these, collagen offers particular advantages, including the presence of biochemical cues that support cell attachment, proliferation, migration and differentiation. Collagen has been co-polymerized with other naturally derived materials in order to improve their biofunctionality. Moreover, they degrade without the release of harmful by-products.

One of the major challenges in the development of biomaterials for osteochondral application is to adequately mimic the gradient structure of natural osteochondral tissue with distinct but seamlessly integrated layers appropriately designed to repair bone, calcified cartilage and articular cartilage. The first generation of constructs involved fabrication of two separate scaffolds: one designed to repair the cartilage tissue and the other designed to repair bone tissue. These two scaffolds were subsequently fused together using sutures [24,25] or biological sealants or glues [19,26,27]. The success of such materials has been limited due to poor cellular infiltration through the layers of the structure. In addition, such bilayered scaffolds were not designed to regenerate the calcified cartilage region which forms the interface between the bone and cartilage regions of osteochondral tissue and plays an important functional role in the prevention of vascular invasion from bone into cartilage. The absence of a calcified cartilage region results in an unstable interface, which can result in bony ingrowth into the cartilage region of the defect space [28].

The approach used in the current study builds on our research group's expertise in the development of collagen-based biomaterials for tissue regeneration. This study set out to develop a collagen-based multi-layered scaffold with distinct but seamlessly integrated layers that mimic the structure and composition of osteochondral tissue while also showing potential for use clinically as a cell-free scaffold that would allow the attachment, proliferation and infiltration of the host's own cells recruited from the bone marrow. We hypothesized that an ideal scaffold for osteochondral repair could be produced by combining a base layer consisting of a collagen–hydroxyapatite (HA) scaffold exhibiting osteoinductive properties and potential for bone repair [29] with a collagen–HA–glycosaminoglycan intermediate calcified cartilage layer and finally a pro-chondrogenic collagen–hyaluronic-acid-based cartilaginous layer [30].

The study aimed to investigate the structural and micro-architectural properties of the final construct and in addition to assess the biological performance of the scaffold *in vitro*, determining the biocompatibility of the scaffold, the attachment and proliferation of cells on the scaffold and the ability of cells to infiltrate through the porous architecture and distribute evenly throughout the construct.

2. Materials and methods

In order to fabricate the multi-layered osteochondral scaffold, a series of preliminary experiments was carried out. These include investigations into different methods of hydration and lyophilization of the individual scaffold layers prior to the addition of the overlying layers, distinct freezing regimes, to enable complete freezing of the collagen-based suspensions, as well as various drying programmes to ensure complete drying of the scaffold. The optimized method, termed the iterative layering fabrication method, illustrated in Fig. 1, is described here.

2.1. Scaffold fabrication

2.1.1. Preparation of collagen-based suspensions

2.1.1.1. Bone layer suspension. The bone-mimicking region of the scaffold was based on a novel bone repair scaffold, HydroxyColl [31], which was previously developed within our group and is currently being commercialized by a campus spin-out company under the trade name SurgaColl Technologies. The HydroxyColl scaffold is composed of type I collagen and HA and was prepared as described previously [29]. Briefly, microfibrillar bovine tendon type I collagen (Col1) (Collagen Matrix Inc., NJ, USA) was blended with 0.5 M acetic acid solution (pH 2.8) for 90 min in a cooled reaction vessel using an IKA Ultra Turrax T18 overhead blender (IKA Works Inc., Wilington, NC) at a speed of 15,000 rpm. HA powder (Captal "R" Reactor Powder, Plasma Biotal, UK) was suspended in 0.5 M acetic acid solution and added in aliquots to the collagen suspension every hour during blending to give a collagen–HA (CHA) suspension with a final collagen concentration of 0.5% (w/v) and HA concentration of 1% (w/v).

2.1.1.2. Intermediate layer suspension. The intermediate layer suspension is composed of type I collagen (Col1), type II collagen (Col2) (porcine type 2 collagen, Biom'up, Lyon, France) and HA. Col1 (0.5% (w/v)) and Col2 (0.5% (w/v)) were blended in 0.5 M acetic acid. The HA was added similarly to the bone layer suspension described above, to give a HA concentration of 0.2% (w/v).

2.1.1.3. Cartilage layer suspension. The cartilage mimicking layer contains Col1, Col2 and hyaluronic acid sodium salt derived from streptococcus equi (HyA) (Sigma–Aldrich, Arklow, Ireland). The suspension was produced by blending Col1 (0.125% (w/v) and Col2 (0.375% (w/v) in 0.5 M acetic acid for 90 min. HyA was dissolved in 0.5 M acetic acid, using a previously developed method [30], and subsequently added into the Col1:Col2 suspension at a concentration of 0.05% (w/v). Following blending, suspensions were degassed under a vacuum of 10 mbar for 10 min.

2.1.2. Iterative layering fabrication process

The bone layer scaffold was fabricated using a previously described optimized freeze-drying method [29]. Briefly, 15.6 ml of the bone layer suspension was pipetted into a stainless-steel tray (internal dimensions, 60 mm × 60 mm) and subsequently placed into a freeze-dryer (Virtis Genesis 25EL, Biopharma, Winchester, UK). This was then freeze-dried at a constant cooling rate of 1 °C min^{-1} to a final freezing temperature of −40 °C [9,32]. Following freeze-drying, the scaffold was crosslinked using a 1-ethyl-3–3-dimethyl aminopropyl carbodiimide (EDAC)/N-hydroxysuccinimide (NHS) (Sigma–Aldrich, Arklow, Ireland) using a concentration of 6 mM EDAC g^{-1} of collagen and a 5:2 M ratio of EDAC:NHS [33]. Crosslinking was carried out for 2 h at room temperature, after which scaffolds were rinsed several times to eliminate water soluble urea, which is a by-product of the reaction. This crosslinking step improves the bulk stiffness of the base layer in order to provide it with sufficient structure to support the addition of the overlying intermediate layer.

The crosslinked bone layer scaffold was subsequently hydrated using 0.025 M acetic acid solution within the stainless steel tray. The 0.025 M acetic acid acts as a support to the bone layer scaffold during addition of the next layer and also enables thermal

Please cite this article in press as: Levingstone TJ et al. A biomimetic multi-layered collagen-based scaffold for osteochondral repair. Acta Biomater (2014), http://dx.doi.org/10.1016/j.actbio.2014.01.005

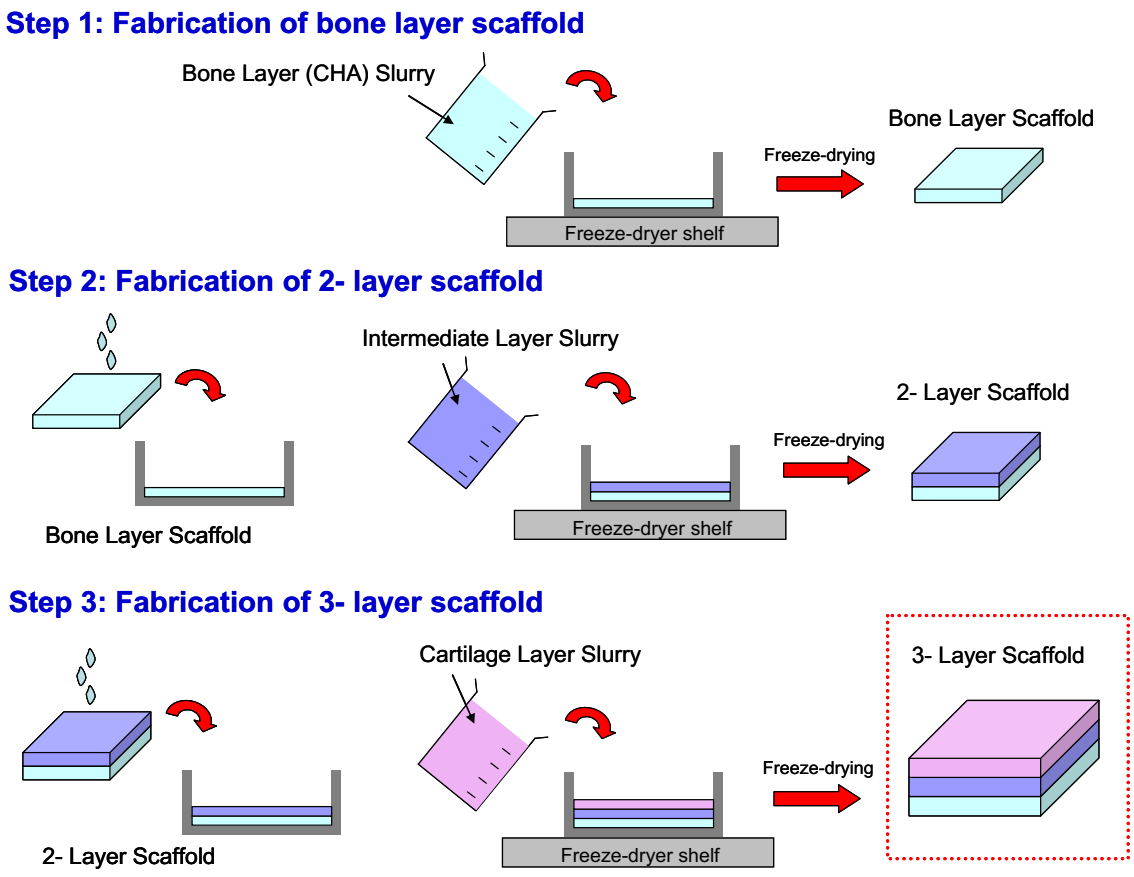

Fig. 1. Iterative layering fabrication process diagram. The iterative layering process is a three-step process which allows the material composition and scaffold micro-architecture in each region of the scaffold to be specifically tailored while producing a resultant scaffold with a seamlessly integrated layer structure.

conduction through the pre-formed scaffold. The second layer was then added by pipetting 7.8 ml of the intermediate layer suspension on top of the hydrated bone layer scaffold and freeze-drying using a similar protocol as before at a constant freezing rate of 1 °C min^{-1} to a final freezing temperature of −40 °C. This resulted in a highly porous two-layer scaffold composed of the bone layer and intermediate layer.

The rehydration process described above was repeated for the two-layer scaffold prior to the addition of 15.6 ml of the cartilage layer suspension. This was then freeze-dried using a freeze-drying cycle similar to that already described: a constant freezing rate of 1 °C min^{-1} and a final freezing temperature of −40 °C, but with the inclusion of prolonged freezing and drying steps to ensure optimal freeze-drying of the construct. This was carried out based on preliminary work which indicated that poor micro-structural properties and incomplete drying resulted when using the standard freeze-drying protocol. A thermocouple probe was placed in each collagen suspension during the freeze-drying cycle in order to monitor the thermal profile. The fabrication process is summarized in Fig. 1.

Following freeze-drying, the porous three-layer scaffolds underwent dehydrothermal (DHT) treatment in a vacuum oven (Vacucell 22; MMM, Germany) at a temperature of 105 °C under a vacuum of 0.05 bar for 24 h. This was carried out to create cross-links through a condensation reaction which results in amide bonds. In addition, the process also sterilized the scaffolds prior to *in vitro* assessment. Cylindrical scaffold samples of 9.5 mm diameter were cut from the scaffold sheet using a metal punch for further analysis.

2.2. Scaffold characterization

Analysis was carried out on the final three-layer scaffold and also on the individual component layers of the scaffold. In addition, a collagen-only single layer scaffold fabricated using the standard −40 °C freeze-drying recipe was used as a control in this study [34]. This collagen-only control was selected in order to allow the effect of adding components such as Col2, HyA and HA to be determined. All scaffolds were sterilized using a DHT treatment method in a vacuum oven (Vacucell 22; MMM, Germany) at a temperature of 105 °C under a vacuum of 0.05 bar for 24 h prior to testing.

2.2.1. SEM analysis

The scaffold micro-architecture was analysed using scanning electron microscopy (SEM) (JEOL 840 73, Joel, Japan). Samples were mounted on sample holders and placed in a SEM chamber without prior addition of a sputter coating. Scan settings of 15 keV and 3×10^{-10} A were used.

2.2.2. Porosity

The porosity of each of the component layers of the three-layer scaffold was determined using a method based on the relative density of the freeze-dried material [29]. Scaffold volume was determined by measuring the sample dimensions using vernier callipers, and the mass using a mass balance. The relative density of the scaffolds was calculated and the percentage porosity was calculated using Eq. (1):

$$\text{Porosity}(\%) = (1 - \rho_{\text{scaffold}}/\rho_{\text{solid}}) \times 100 \quad (1)$$

Please cite this article in press as: Levingstone TJ et al. A biomimetic multi-layered collagen-based scaffold for osteochondral repair. Acta Biomater (2014), http://dx.doi.org/10.1016/j.actbio.2014.01.005

2.2.3. Scaffold pore size

Scaffold pore structure and pore size analysis was carried out using a technique described previously [9]. Scaffold samples were embedded in JB-4 glycolmethacrylate (Polysciences Europe, Eppelheim, Germany) and then sectioned using a microtome (Leica RM 2255, Leica, Germany) to provide sections of 10 μm in thickness. These were mounted on slides and stained using toluidine blue (Sigma–Aldrich, Arklow, Ireland). Digital images were captured at a magnification of 10 × using a microscope (Eclipse 90i, Nikon, Japan) and a digital camera (DS Ri1, Nikon, Japan). Pore size analysis was carried out using a MATLAB (MathWorks Inc, MA, USA)-based pore topology analyser programme previously described [34]. The programme converts the digital images into binary form and calculates the average pore size based on the best fit elliptical lengths generated by the software.

2.2.4. Mechanical testing

The mechanical properties were assessed through unconfined compression testing using a Zwick Z050 mechanical testing machine and integrated testing software testXpert (Zwick/Roell GmbH, Ulm, Germany). Scaffold samples were prehydrated in phosphate buffered saline (PBS) for 1 h prior to testing and immersed in PBS throughout the tests. Testing was carried out using a 5 N load cell at a strain rate of 10% min^{-1}, up to a maximum of 10% strain. The compressive modulus was defined as the slope of a linear fit to the stress–strain curve over 2–5% strain [34,35].

2.2.5. Interfacial adhesion strength

Interfacial adhesion strength between the layers of the construct was determined using a custom-designed interfacial strength test rig fitted to a Zwick Z050 Mechanical Testing Machine (Zwick/Roell GmbH, Ulm, Germany). The rig design allows the secure fixation of the scaffold during testing while ensuring correct alignment of the scaffold between the machine's load cell and base platen. Scaffold samples were adhered to aluminium test stubs using a high viscosity adhesive (Araldite, Radionics, Ireland) and inserted into the rig for testing. The high viscosity of the adhesive used ensured minimal integration into the scaffold. This was confirmed by applying the adhesive to the scaffold and inspecting the depth of penetration following sectioning. Samples were hydrated in PBS for 1 h prior to testing to failure using a 5 N load cell under a tensile load applied at a strain rate of 10% min^{-1}. Failure was expected to occur either at the ultimate tensile strength of one of the component layers of the scaffold or as a result of delamination at the layer interfaces.

2.3. In vitro analysis

In vitro analysis was carried out in order to assess scaffold biocompatibility, cellular attachment and the ability of cells to infiltrate through the layered structure of the scaffold. Scaffold discs, 12.7 mm (½″) in diameter and 4 mm in height, were seeded with MC3T3-E1 mouse pre-osteoblast cells (ATCC-LGC, Teddington, Middlesex, UK) at a density of 1×10^6 cells per scaffold. Cell-seeded scaffolds were cultured in alpha-minimum essential medium (α-MEM) (Biosera, Ringmer, UK) supplemented with 2% penicillin/streptomycin (Sigma–Aldrich, Arklow, Ireland), 1% L-glutamine (Sigma–Aldrich, Arklow, Ireland) and 10% fetal bovine serum (Biosera, Ringmer, UK) at 37 °C and 5% CO_2 and evaluated at 7 and 14 days post seeding. In order to determine scaffold viability, cell number was determined by DNA quantification using a Hoechst DNA assay (Sigma–Aldrich) ($n = 4$). Scaffolds were homogenized with 1 ml Qiazol (Qiagen, Crawley, UK) using a hand-held homogenizer (Finemech, Portola Valley, CA, USA). Cell number was quantified using a fluorescent Hoechst dye 33 258 assay as previously described [8]. Measurements were taken from a fluorometric plate reader (Wallac 1420 Victor2 D, Perkin Elmer, MA, USA) at an emission of 460 nm and excitation of 355 nm, 1.0 s. The measurements were read against a standard curve to obtain the relative cell numbers per scaffold in terms of the DNA content.

Histological analysis was carried out in order to evaluate how effectively cells infiltrated through the layered constructs. Constructs were fixed in 10% formalin for 2 h and then processed in an automatic tissue processor (ASP300, Leica, Wetzlar, Germany). Constructs were then embedded in paraffin wax and sectioned at a thickness of 10 μm using a rotary microtome (RM2255, Leica microtome, Leica). Sections were stained using hematoxylin and eosin (H&E) staining and digital images captured in order to evaluate cell infiltration through the scaffold.

2.4. Statistical analysis

Data are presented as mean standard deviation. Differences between two treatments were assessed using the student's paired t-test and between three or more were assessed using one-way ANOVA. Statistical significance was taken at $p < 0.05$.

3. Results

3.1. Analysis of scaffold architecture

The homogeneous pore structure produced by the freeze-drying process was demonstrated using scanning electron microscopy (SEM) analysis of the three-layer scaffold as shown in Fig. 2. A high degree of pore interconnectivity throughout the construct can be observed. Structural continuity at the interfaces was evident, with the individual layers being seamlessly integrated. This seamless integration of the scaffold layers is vital in order to promote cell infiltration and the regeneration of tissue in the different layers of the scaffold.

Scaffold porosity was found to be >98.8% for each of the component layers of the three-layered scaffold. A reduction in porosity was seen in scaffolds containing HA; however, this reduction (from 99.5% for collagen-only control to 98.8% for bone layer scaffold) was negligible. Layered scaffolds fabricated using the iterative layering technique maintained the highly porous structure observed for the constituent layers when fabricated independently. Investigation of the scaffold pore architecture demonstrated the homogeneous pore structure present within the scaffold (Fig. 3a). Measurement of pore size revealed an average pore diameter of 126 μm in the cartilage layer, 112 μm in the intermediate layer and 136 μm in the bone layer, as shown in Fig. 3b. There was no significant difference in the pore size of the bone and cartilage regions compared to the collagen-only control scaffold. The mean pore size in the intermediate layer was found to be smaller than that of the bone and cartilage layers ($p < 0.05$, $n = 4$).

3.2. Assessment of scaffold mechanical properties

The compressive moduli of the constituent layers of the scaffold and of the combined three-layer scaffold are compared in Fig. 4. The bone layer was found to have the highest compressive modulus of ~0.95 kPa, significantly higher than the other two groups ($p < 0.05$). This is due to the presence of the HA mineral phase in this layer. The compressive moduli of the collagen control, the intermediate layer and the cartilage layer were found to be ~0.4 kPa, 0.35 kPa and 0.3 kPa, respectively. The compressive modulus of the three-layer scaffold was found to be 0.51 kPa. No statistically significant difference ($p > 0.05$) was found between these groups.

Please cite this article in press as: Levingstone TJ et al. A biomimetic multi-layered collagen-based scaffold for osteochondral repair. Acta Biomater (2014), http://dx.doi.org/10.1016/j.actbio.2014.01.005

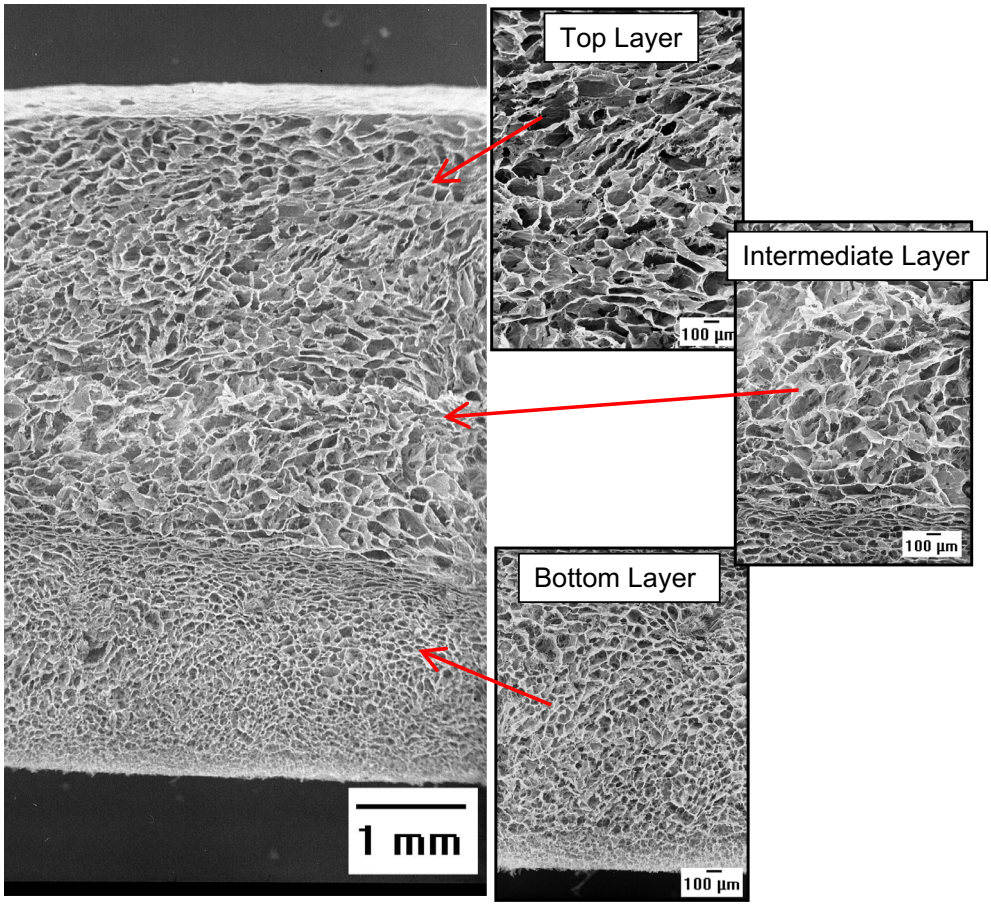

Fig. 2. Representative SEM micrographs of the three-layer scaffold showing the highly porous structure, high degree of pore interconnectivity and seamless integration of the component layers.

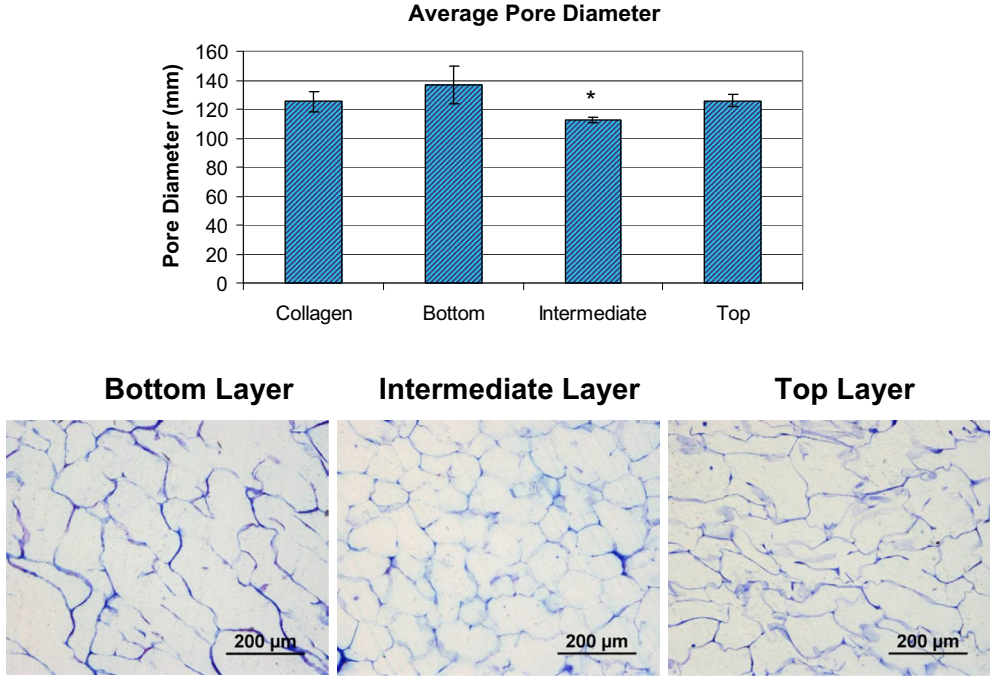

Fig. 3. (a) Comparison of the pore diameters of each of the component layers of the three-layer scaffold produced in isolation (*$p > 0.05$, $n = 4$). The average pore diameters were found to vary from 112 µm (intermediate layer scaffold) to 136 µm (bottom layer scaffold). (b) Representative micrographs of the pore structure of each of the component layers of the three-layer scaffold. The micrographs show the homogeneous pore architecture in each region of the scaffold.

Please cite this article in press as: Levingstone TJ et al. A biomimetic multi-layered collagen-based scaffold for osteochondral repair. Acta Biomater (2014), http://dx.doi.org/10.1016/j.actbio.2014.01.005

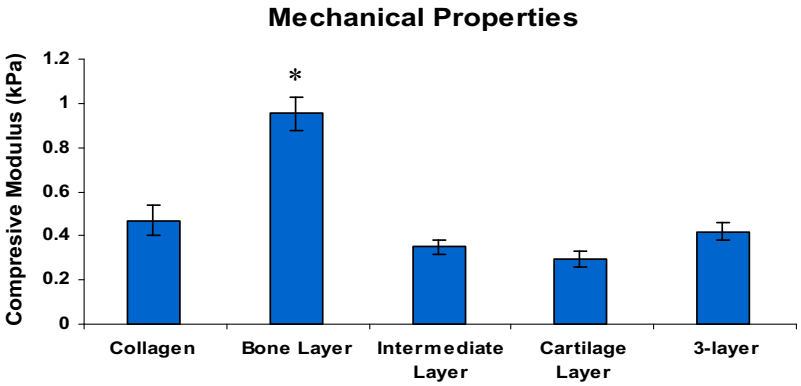

Fig. 4. Effect of the layering process on mechanical properties of scaffolds following DHT treatment at 105 °C for 24 h (*$p > 0.05$, $n = 6$). The presence of HA in the bone layer led to an increase in the compressive modulus. The compressive modulus of the three-layer scaffold was found to be 0.51 ± 0.03 kPa. No significant difference was found between the collagen control scaffold, the intermediate layer, the cartilage layer or the three-layer scaffold, indicating that the iterative layering process does not negatively affect scaffold mechanical properties.

The interfacial adhesion strength for the two-layer (bone and intermediate layers) and three-layer (bone, intermediate and cartilage layers) scaffolds fabricated using the iterative layering technique are shown in Fig. 5. Delamination of the different layers was not observed during testing. Failure occurred within the intermediate layer in the two-layer scaffold and within the cartilage layer in the three-layer scaffold showing that the interfacial strength was greater than the tensile strength of the individual layers themselves. The tensile properties were lower for the three-layer scaffold than the two-layer scaffold due to the presence of type II collagen in the cartilage layer of the three-layer scaffold. Fibre pullout was observed on the fracture surface following testing, indicating integration between the scaffold layers.

3.3. In vitro assessment

Biocompatibility was assessed by quantifying cell number within the three-layer scaffolds and a collagen-only control scaffold. No significant difference in cell number was found between the two groups at day 7 post seeding (Fig. 6a). There was an increase of ~50% in cell number from day 0 to day 7 and a further 50% increase by day 14 for both the collagen control and the three-layer scaffolds. The homogeneous distribution of cells within the porous structure of the three-layer scaffold was observed following analysis of H&E stained histological sections at 14 days post seeding (Fig. 6b). No encapsulation effect was observed from this analysis. Cellular infiltration through all three layers of the construct was evident, thus confirming the seamless integration at the interfaces of the individual layers.

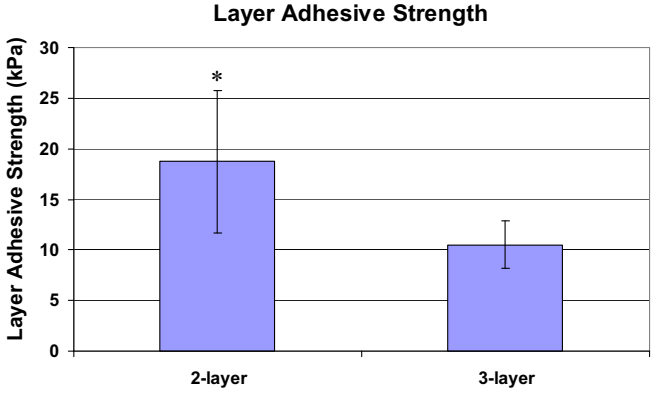

Fig. 5. Layer adhesion strength test results for the two-layer (bone and intermediate layers) and three-layer (bone, intermediate and cartilage layers) scaffolds fabricated using the iterative layering technique (*$p > 0.05$, $n = 8$). In all cases, delamination was not seen at the interfaces. Instead, failure occurred within the intermediate layer in the two-layer scaffold and within the cartilage layer in the three-layer scaffold, showing that the interfacial strength was greater than the tensile strength of the materials used. The tensile properties were lower for the three-layer scaffold than the two-layer scaffold due to the presence of type II collagen in the cartilage layer of the three-layer scaffold.

4. Discussion

Due to the complex zonal organization of osteochondral tissue, the development of a single implantable biomaterial with a gradient structure is of great interest in the field of osteochondral tissue engineering [36,37]. This study built on the existing collagen-based scaffold expertise within our research group to develop a novel multi-layered material for osteochondral repair. The resultant scaffold contains three distinct regions appropriately designed for the repair of the chondral, calcified cartilage and subchondral bone layers present within healthy osteochondral tissue. Through the development of the novel iterative layering manufacturing process, the layered construct described here can be produced without many of the limitations of existing technologies for osteochondral repair, while retaining the core ability to completely tailor each region to provide the optimal cues to enable regeneration of the local tissue within the defect. Collagen forms the base material for each of the layers of this multi-layer construct, thus offering the advantage of the presence of natural binding sites and the ability to degrade without release of harmful degradation products. By combining these biocompatible characteristics, optimized pore structure and mechanical environment, with individually tailored composition within each respective layer, this novel multilayered scaffold has the potential to offer a cell-free "off-the-shelf" approach to osteochondral defect healing. A patent on the technique described to fabricate these scaffolds has been filed [38] and the scaffold itself is currently being commercialized through a spin out campus company, SurgaColl Technologies under the trade name ChondroColl. As well as showing potential in the fabrication of a construct for use in osteochondral repair, the methodology described could also be applied for the fabrication of scaffolds for other applications involving the repair and regeneration of multi-layered biological tissues.

The material composition of each layer of the scaffold was designed taking into account the native extracellular matrix (ECM) of osteochondral tissue. The superficial layer of articular cartilage, which is composed of a rich glycosaminoglycan content and type II collagen, the cartilage layer of the scaffold was fabricated from type I collagen, type II collagen and hyaluronic acid. Type II

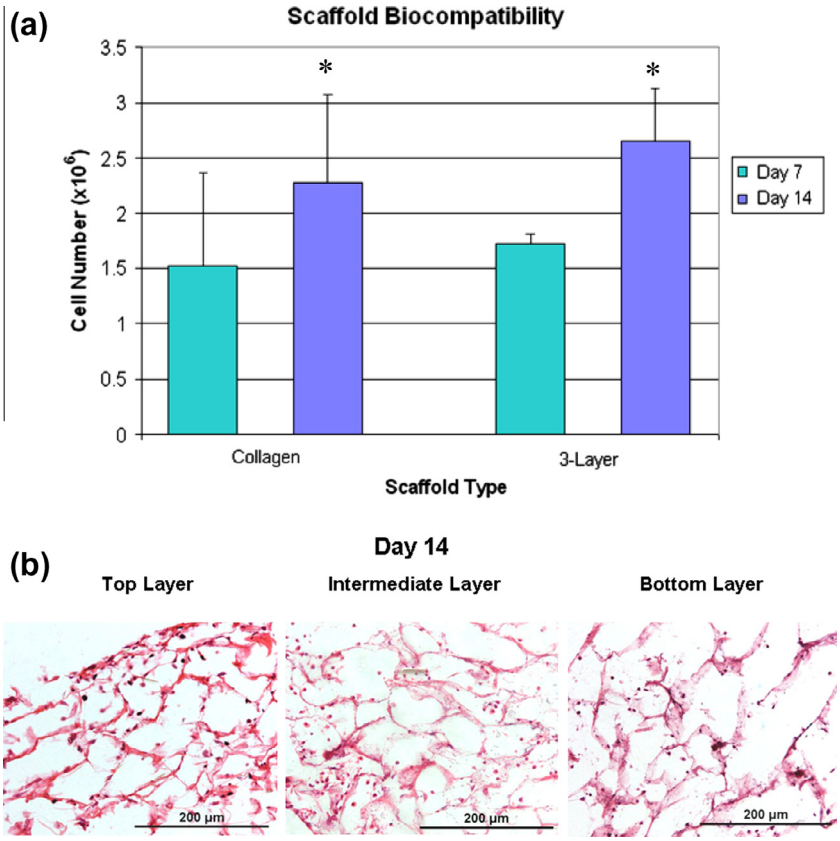

Fig. 6. (a) Cell numbers for three-layer scaffolds compared to collagen scaffolds at 7 and 14 days (*$p > 0.05$, $n = 5$). Cell numbers were seen to increase by ~50% from day 7 to day 14 for both the collagen and the three-layer scaffolds. The ability of cells to proliferate within the three-layer scaffold indicates the biocompatible nature of the scaffold. (b) Histologically prepared, H&E stained transverse sections of the three-layer scaffold following 14 days *in vitro* culture with MC3T3-E1 mouse pre-osteoblast cells. Infiltration of cells was seen throughout the full scaffold structure at this time point. Hemotoxylin stained nuclei are indicated by the arrows.

collagen and hyaluronic acid have previously shown the potential to induce and maintain MSC chondrogenesis within the literature and previous investigations carried out by our group [30,39,40]. Preliminary work in our laboratory demonstrated that scaffolds fabricated from type II collagen and hyaluronic acid had poor mechanical properties with subsequent difficulty in handling. However, the incorporation of collagen type I significantly increased the mechanical properties of the cartilage layer. Type I collagen scaffolds have been previously shown in our laboratory to support the chondrogenic differentiation of rat bone marrow MSC cells [41]. The calcified cartilage or tidemark region of native osteochondral tissue is hypothesized to prevent ingrowth of bone into the chondral region in the defect space; a problem frequently observed following implantation of earlier two-layer osteochondral repair materials [28]. The intermediate layer of the three-layer scaffold developed here replicates the composition of the calcified cartilage region, containing type I collagen, type II collagen and HA.

Similar to the two overlying layers, the bone layer of the triphasic scaffold was designed to mimic the native composition of subchondral bone ECM: type I collagen and HA. This layer was found to possess an interconnected pore architecture (Fig. 3b), significantly higher compressive modulus than the cartilage and intermediate layers (Fig. 4) as well as homogeneous cellular distribution following 14 days of culture *in vitro* (Fig. 6b). Due to the higher compressive modulus of subchondral bone compared to articular cartilage, we designed this multi-layered scaffold with a view to having an increasing gradient of stiffness from the cartilage layer to the bone layer. The addition of HA (1% w/v) to collagen led to a significant increase in the bulk compressive modulus of the bone layer. A number of studies have shown that the stiffness of substrates can mediate the lineage that undifferentiated cells follow [10,42]. Indeed, studies within our laboratory have shown that collagen-based scaffolds with stiffer substrates can support initiation of MSC osteogenic differentiation in the absence of growth factors [11]. In this context, having the bottom bone layer with the highest compressive modulus may encourage the osteogenic differentiation of progenitor cells. Moreover, the presence of HA particles within this layer, which have been shown to be osteo-inductive both *in vitro* and *in vivo* [29,43], will also enhance the osteogenic differentiation, thus, enhancing its role in the zonal organization of regenerated osteochondral tissue.

The micro-structural and mechanical properties of a tissue engineered construct have a significant impact on cellular differentiation. The pore size in freeze-dried materials is dependent on the freeze-drying parameters used in the fabrication process. To achieve a homogeneous pore structure, conduction of thermal energy between the material being freeze-dried and the freeze-dryer shelf is essential [32]. When freeze-drying a layered material there is no direct contact between the overlying layer and the base of the tray. To overcome this limitation, the rehydration of the bone layer was found to facilitate the transfer of thermal energy through the bone layer and to enable the desired ice crystal formation during freezing. This enabled control of the pore size within each region of the scaffold. Indeed, optimization of the pore structure is crucial since it has been shown that scaffold mean pore size has a considerable effect on the response of seeded cells. In particular, Murphy et al. [8] showed that both cellular attachment and infiltration are significantly affected by scaffold mean pore size. In addition, research within our laboratory has also shown that scaffold mean pore size has a deterministic role in cell differentiation and matrix deposition.

Please cite this article in press as: Levingstone TJ et al. A biomimetic multi-layered collagen-based scaffold for osteochondral repair. Acta Biomater (2014), http://dx.doi.org/10.1016/j.actbio.2014.01.005

Seamless integration between the layers is essential in order to support our paradigm which proposes to utilize and encourage the infiltration of the host's own cells from the bone marrow through all regions of the scaffold. We propose that once sufficient infiltration is achieved, the local availability of pro-osteogenic/chondrogenic moieties provided by the scaffold (substrate stiffness, architecture, composition) would support the generation of layer-specific ECM, providing an ideal environment to encourage early-stage de novo tissue development. SEM investigation (Fig. 2) enabled the interfacial regions to be visualized, with layer interfaces between the individual layers difficult to distinguish, thus confirming the achievement of seamless integration between each individual layer through use of this iterative layering process. To investigate the stability of the integrated layers, interfacial strength at the interfaces between each layer was assessed. Poor interfacial strength leads to delamination of the layers, a problem widely reported in the fabrication of layered scaffold materials for tissue engineering [15,26,27]. Using a custom layer adhesion strength measurement technique, the interfacial layer strength was tested to failure, with delamination of the layers being found to occur within the confines of the mechanically weakest layer (top cartilage layer) rather than at the interface. This supports the earlier assessment of seamless integration of the layers, evident by the interfaces' superior strength compared to the individual layers themselves. Subsequent examination of the fracture surfaces following testing exhibited fibre pullout, indicating that a bridging of the fibre structure occurs across the interfaces as a result of the novel manufacturing process. This process thus provides an ideal composite structure which maximizes layer bonding strength without the need for glues or sutures.

Substrate stiffness also plays a role in the direction of MSC differentiation, with stiffer scaffolds showing differentiation of cells towards an osteogenic lineage and less stiff matrices directing MSCs towards a chondrogenic lineage [11]. The iterative layering process allows the tailoring of stiffness in each region of the multi-layer scaffold (Fig. 4). Having previously optimized the substrate stiffness for osteogenesis and chondrogenesis within these collagen-based constructs, the retention of a seamless pore structure throughout the material but coupled with the customizable substrate stiffness, via compositional changes or subsequent cross-linking methodologies, provides a significant amount of flexibility to maximize the potential of this novel scaffold for use in osteochondral defect repair.

The ability of cells to attach to and proliferate on the multi-layer scaffold as evidenced during *in vitro* assessment demonstrates the biocompatibility of the scaffold. Little difference in cell number was observed between the multi-layer construct and the control collagen scaffold, indicating that the osteogenic and chondrogenic components added during fabrication do not affect the biocompatibility of the scaffold. A highly porous material with an interconnected pore structure is essential in order for cells to infiltrate through a material, attach to it and begin the deposition of matrix. The layered scaffold produced using the iterative layering technique described here has a porosity of >97%. This is marginally lower than the porosity of each of the constituent layers when fabricated as separate scaffolds, demonstrating that the process of layering and freeze-drying has minimal detrimental effect on the porosity of the material. Homogenous cellular distribution throughout the entire construct was demonstrated *in vitro* (Fig. 6b), indicating that the seamless layer integration allows cellular infiltration through the construct and confirms that the scaffold has the potential to allow host cells to distribute evenly throughout the scaffold's gradient structure following implantation *in vivo*. The *in vitro* investigation described here indicates the biocompatibility of the scaffold and ability of cells to infiltrate the porous structure of the scaffold. The *in vivo* environment is more complicated, with a range of cell types from the blood and bone marrow infiltrating the scaffold following implantation. The scaffold is expected to initially provide a site for blood clot formation, and following the natural inflammatory response and influx of cells, to provide a template that guides the generation of repair tissue. In order to more fully understand this process and the regenerative potential of the scaffold, *in vivo* investigation is required. This is the focus of ongoing studies in our laboratory. Taken together, these results show the potential of this multi-layered scaffold as an advanced strategy for osteochondral defect repair.

5. Conclusions

In summary, this study has developed a novel, seamlessly integrated tissue engineering scaffold for osteochondral repair. The resultant scaffold mimics the inherent gradient structure of healthy osteochondral tissue, containing a bone layer, an intermediate layer and a cartilaginous layer. The iterative layering technique described here has shown advantages over previously reported layered scaffold fabrication techniques in terms of the potential for optimization of the composition, pore size, porosity and mechanical properties of each individual layer of the multi-layered scaffold. As well as showing potential in the fabrication of a construct for use in osteochondral repair, the methodology described can also be applied for the fabrication of scaffolds for other applications involving the repair and regeneration of multi-layered biological tissues. This novel scaffold provides an optimized environment for cell attachment and proliferation due to a seamlessly integrated layer structure, high levels of porosity, a homogeneous pore structure and a high degree of pore interconnectivity, all of which are essential in order to allow cellular infiltration, diffusion of nutrients, removal of waste and to promote regeneration of seamless anatomical repair tissue. These results suggest that this novel material has considerable promise as a scaffold for osteochondral repair.

Conflict of interest

J.P.G. is the Chief Executive Officer in SurgaColl Technologies, a spin-out campus company that has recently licensed the multi-layer scaffold described in this work. The authors did not receive any financial support from SurgaColl Technologies for this project.

Acknowledgements

The authors acknowledge Enterprise Ireland Proof of Concept Award (PC/2007/331) and Commercialisation Fund Technology Development Award (CFTD/2009/0104) and a Translational Research Award from the Irish Health Research Board/Science Foundation Ireland TRA/2011/19 for funding.

Appendix A. Figures with essential colour discrimination

Certain figures in this article, particularly Figs. 1–6, are difficult to interpret in black and white. The full colour images can be found in the on-line version, at http://dx.doi.org/10.1016/j.actbio.2014.01.005.

References

[1] Hunziker EB. Articular cartilage repair: basic science and clinical progress. A review of the current status and prospects. Osteoarthritis Cartilage 2001;10:432–63.

[2] Vijayan S, Bentley G, Briggs TWR, Skinner JA, Carrinfton RWJ, Pollock R, et al. Cartilage repair: a review of Stanmore experience in the treatment of osteochondral defects in the knee with various surgical techniques. Indian J Orthop 2010;44:238–45.

[3] Bekkers JEJ, deWindt ThS, Brittberg M, Saris DBF. Cartilage repair in football (soccer) athletes: what evidence leads to which treatment? A critical review of the literature. Cartilage 2012;3:43S–9S.
[4] Cole BJ, Pascual-Garrido C, Grumet RC. Surgical management of articular cartilage defects in the knee. J Bone Joint Surg Am 2009;91:1778–90.
[5] Smith GD, Knutsen G, Richardson JB. A clinical review of cartilage repair techniques. J Bone Joint Surg Am 2005;87-B:445–9.
[6] Horas U, Pelinkovic D, Herr G, Aigner T, Schnettler R. Autologous chondrocyte implantation and osteochondral cylinder transplantation in cartilage repair of the knee joint: a prospective, comparative trial. J Bone Joint Surg Am 2003;85-A:185–92.
[7] Hangody L, Dobos J, Balo E, Panics G, Hangody LR, Berkes I. Clinical experiences with autologous osteochondral mosaicplasty in an athletic population: a 17-year prospective multicenter study. Am J Sports Med 2010;38:1125–33.
[8] Murphy CM, Haugh MG, O'Brien FJ. The effect of mean pore size on cell attachment, proliferation and migration in collagen glycosaminoglycan scaffolds for tissue engineering. Biomaterials 2010;31:461–6.
[9] O'Brien FJ, Harley BA, Yannas IV, Gibson LJ. The effect of pore size on cell adhesion in collagen–GAG scaffolds. Biomaterials 2005;26:433–41.
[10] Engler AJ, Sen S, Sweeney HL, Discher DE. Matrix elasticity directs stem cell lineage specification. Cell 2006;126:677–89.
[11] Murphy CM, Matsiko A, Haugh MG, Gleeson JP, O'Brien FJ. Mesenchymal stem cell fate is regulated by the composition and mechanical properties of collagen–glycosaminoglycan scaffolds. J Mech Behav Biomed 2012;11:53–62.
[12] Abrahamsson CK, Yang F, Park H, Brunger JM, Valonen PK, Langer R, et al. Chondrogenesis and mineralization during *in vitro* culture of human mesenchymal stem cells on three-dimensional woven scaffolds. Tissue Eng A 2010;16:3709–18.
[13] Schaefer D, Martin I, Jundt G, Seidel J, Heberer M, Grodzinsky AJ, et al. Tissue engineered composites for the repair of large osteochondral defects. Arthritis Rheum 2002;46:2524.
[14] Chang NJ, Lin CC, Li CF, Wang DA, Issariyaku N, Yeh ML. The combine effects of continuous passive motion treatment and acellular PLGA implants on osteochondral regeneration in the rabbit. Biomaterials 2012;33:3153–63.
[15] Sherwood JK, Riley SL, Palazzolo R, Brown SC, Monkhouse DC, Coates M, et al. A three-dimensional osteochondral composite scaffold for articular cartilage repair. Biomaterials 2002;23:4739–51.
[16] Marquass B, Somerson JS, Hepp P, Aigner T, Schwan S, Bader A, et al. A novel MSC-seeded triphasic construct for the repair of osteochondral defects. J Orthop Res 2010;12:1586–99.
[17] Ito Y, Adachi N, Nakamae A, Yanada S, Ochi M. Transplantation of tissue-engineered osteochondral plug using cultured chondrocytes and interconnected porous calcium hydroxyapatite ceramic cylindrical plugs to treat osteochondral defects in a rabbit model. Artif Organs 2008;32:36–44.
[18] Brittberg M, Sjögren-Jansson E, Lindahl A, Peterson L. Influence of fibrin sealant (Tisseel®) on osteochondral defect repair in the rabbit knee. Biomaterials 1997;18:235–42.
[19] Gao J, Dennis JE, Solchaga LA, Awadallah AS, Goldberg VM, Caplan AI. Tissue-engineered fabrication of an osteochondral composite graft using rat bone marrow-derived mesenchymal stem cells. Tissue Eng 2001;7:363–71.
[20] Igarashi T, Iwasaki N, Kasahara Y, Minami A. A cellular implantation system using an injectable ultra-purified alginate gel for repair of osteochondral defects in a rabbit model. J Biomed Mater Res A 2010;94:844–55.
[21] Khanarian NT, Haney NM, Burga RA, Lu HH. A functional agarose–hydroxyapatite scaffold for osteochondral interface regeneration. Biomaterials 2012;33:5247–58.
[22] Hung CT, Lima EG, Mauck RL, Taki E, LeRoux MA, Lu HH, et al. Anatomically shaped osteochondral constructs for articular cartilage repair. J Biomech 2003;36:1853–64.
[23] Sheehy EJ, Vinardell T, Buckley CT, Kelly DJ. Engineering osteochondral constructs through spatial regulation of endochondral ossification. Acta Biomater 2013;9:5484–92.
[24] Chen G, Tanaka J, Tateishi T. Osteochondral tissue engineering using PLGA–collagen hybrid mesh. Mater Sci Eng 2006;26:124.
[25] Schaefer D, Martin I, Shastri P, Padera RF, Langer R, Freed LE, et al. *In vitro* generation of osteochondral composites. Biomaterials 2000;21:2599–606.
[26] Kreklau B, Sittinger M, Mensing MB, Voigt C, Berger G, Burmester GR, et al. Tissue engineering of biphasic joint cartilage transplants. Biomaterials 1999;20:1743–9.
[27] Niederauer GG, Slivka MA, Leatherbury NC, Korvick DL, Harrof HH, Ehler WC, et al. Evaluation in multiphase implants for repair of focal osteochondral defects in goats. Biomaterials 2000;21:2561–74.
[28] Hunziker EB, Driesang IMK. Functional barrier principle for growth-factor-based articular cartilage repair. Osteoarthritis Cartilage 2003;11:320–7.
[29] Gleeson JP, Plunkett NA, O'Brien FJ. Addition of hydroxyapatite improves stiffness, interconnectivity and osteogenic potential of a highly porous collagen-based scaffold for bone tissue regeneration. Eur Cell Mater 2010;20:218–23.
[30] Matsiko A, Levingstone TJ, O'Brien FJ, Gleeson JP. Addition of hyaluronic acid improves cellular infiltration and promotes early-stage chondrogenesis in a collagen-based scaffold for cartilage tissue engineering. J Mech Behav Biomed 2012;11:41–52.
[31] O'Brien FJ, Gleeson JP, Plunkett NA. Collagen/hydroxyapatite composite scaffold, and process for the production thereof. Patent WO 2008/096334 A2, 2008.
[32] O'Brien FJ, Harley BA, Yannas IV, Gibson L. Influence of freezing rate on pore structure in freeze-dried collagen–GAG scaffolds. Biomaterials 2004;25:1077–86.
[33] Haugh MG, Murphy CM, McKiernan RC, Altenbuchner C, O'Brien FJ. Crosslinking and mechanical properties significantly influence cell attachment, proliferation and migration within collagen glycosaminoglycan scaffolds. Tissue Eng A 2011;17:1201–8.
[34] Haugh MG, Murphy CM, O'Brien FJ. Novel freeze-drying methods to produce a range of collagen–glycosaminoglycan scaffolds with tailored mean pore sizes. Tissue Eng C 2010;16:887–94.
[35] Harley BA, Leung JH, Silva EC, Gibson LJ. Mechanical characterization of collagen–glycosaminoglycan scaffolds. Acta Biomater 2007;3:463–74.
[36] Harley BA, Lynn AK, Wissner-Gross Z, Bonfield W, Yannas IV, Gibson LJ. Design of a multiphase osteochondral scaffold. III. Fabrication of layered scaffolds with continuous interfaces. J Biomed Mater Res B Appl Biomater 2010;92A:1078–93.
[37] Lynn A, Best S, Cameron RE, Harley BA, Yannas IV, Gibson LJ, et al. Design of a multiphase osteochondral scaffold. I. Control of chemical composition. J Biomed Mater Res 2010;92A:1057–65.
[38] Gleeson JP, Levingstone TJ, O'Brien FJ. Layered scaffold suitable for osteochondral defect repair. Patent WO2010/084481, 2009.
[39] Nehrer S, Breinan HA, Ramappa A, Young G, Shortkroff S, Louie LK, et al. Matrix collagen type and pore size influence behaviour of seeded canine chondrocytes. Biomaterials 2007;18:769–76.
[40] Bosnakovski D, Mizuno M, Kim G, Takagi S, Okumura M, Fujinaga T. Chondrogenic differentiation of bovine bone marrow cells (MSCs) in different hydrogels: Influence of collagen type II extracellular matrix on MSC chondrogenesis. Biotechnol Bioeng 2006;93:1152–63.
[41] Farrell E, O'Brien FJ, Doyle P, Fischer J, Yannas I, Harley BA, et al. A collagen–glycosaminoglycan scaffold supports adult rat mesenchymal stem cell differentiation along osteogenic and chondrogenic routes. Tissue Eng 2006;12:459–68.
[42] Discher DE, Janmey P, Wang YL. Tissue cells feel and respond to the stiffness of their substrate. Science 2005;310:1139–43.
[43] Lyons FG, Gleeson JP, Partap S, Coghlan K, O'Brien FJ. Novel Microhydroxyapatite Particles in a Collagen Scaffold: A Bioactive Bone Void Filler?. Clin Orthop Relat Res 2014;310. http://dx.doi.org/10.1007/s11999-013-3438-0. Advance online publication.